Potential neutron-induced γ-ray background on natural tellurium relevant to ^{130}Te $0\nu\beta\beta$ decay searches at the CUORE and SNO+ detectors

W. Tornow* and S. W. Finch
Department of Physics, Duke University, Durham, North Carolina 27708, USA
and Triangle Universities Nuclear Laboratory, Durham, North Carolina 27708, USA

M. F. Kidd
Tennessee Technological University, Cookeville, Tennessee 38501, USA

(Received 15 February 2021; accepted 12 April 2021; published 23 April 2021)

Gamma-ray production cross-section data have been obtained for the inelastic neutron scattering reactions ^{126,128,130}Te$(n, n'\gamma)$ at five neutron energies between 3.6 and 10 MeV. We report data for the γ-ray energy region relevant to $0\nu\beta\beta$ decay of ^{130}Te with a $Q_{\beta\beta}$ value of 2527.515 keV, assuming natural-abundance tellurium, as used at CUORE and SNO+. The natural abundance of ^{130}Te, ^{128}Te, and ^{126}Te is 34%, 32%, and 19%, respectively. For CUORE the γ-ray cascades from the excited state in ^{130}Te at 2527.06 keV and in ^{126}Te at 2533.85 keV are of concern. For SNO+, accounting for its inferior energy resolution, an additional four levels are important in ^{130}Te, an additional nine levels in ^{128}Te, and an additional eight levels in ^{126}Te. Of these, we report neutron-induced γ-ray production cross sections for the strongest transitions: the 2581.15 keV level in ^{130}Te, the 2494.20, 2508.06, and 2630.14 keV levels in ^{128}Te, and the 2496.83 and 2585.46 keV level in ^{126}Te. The largest cross-section values were found for cascade γ-ray transitions to the ground state, while direct transitions to the ground state are very weak and were not observed in the present work. Both the CUORE and SNO+ detectors, however, may not be able to distinguish between cascade transitions and direct transitions to the ground state, making the neutron-induced excitation of the 2527.06 keV state of ^{130}Te in particular a potential problem for $0\nu\beta\beta$ decay searches of ^{130}Te, because it matches its $Q_{\beta\beta}$ value.

DOI: 10.1103/PhysRevC.103.044612

I. INTRODUCTION

Neutrinoless double-beta ($0\nu\beta\beta$) decay is a second-order weak nuclear decay which, if detected, would have large implications for neutrino and particle physics [1]. As such, many large-scale experimental efforts are underway to detect this elusive decay mode. The Cryogenic Underground Observatory for Rare Events (CUORE) collaboration at the Laboratori Nazionali del Gran Sasso (LNGS), Italy, is using natural tellurium in its search for $0\nu\beta\beta$ decay of ^{130}Te (natural abundance 34.1%) [2]. In addition, the SNO+ collaboration at the Sudbury Neutrino Observatory (SNO) located in the Creighton mine in Sudbury, Canada, has started its search for this decay, again using natural tellurium [3]. The CUORE experiment employs 988 TeO_2 bolometers of 750 g each, while the SNO+ experiment is using a large-volume liquid scintillator detector loaded with a tellurium compound at the 0.5% level (natural tellurium by weight), resulting in 1330 kg of ^{130}Te. Although the techniques employed are very different, a common feature of both experiments is related to neutron-induced background, which could mimic the signal of interest. In this paper we investigate prompt γ rays produced by the interaction of fast neutrons on ^{nat}Te.

It is established that cosmic muons can produce neutrons in underground laboratories with energies up to a few GeV [4]. Muon-induced neutrons produced inside the detector may be rejected by using high-efficiency muon vetos. Muon-induced neutrons produced in the rock surrounding the detector, however, can be much more difficult to veto and create a concern for rare-event physics searches such as $0\nu\beta\beta$ decay. This source of neutrons is a larger concern for CUORE, located at LNGS, with an overburden of 3.1 km water equivalent (km.w.e.). SNO+, with an overburden of 6.0 km.w.e., is expected to have a ≈50 times lower muon-induced neutron flux [4].

Another source of neutrons is those produced by (α, n) reactions, caused by actinide contamination internal to the detector and surrounding shielding materials, which produce neutrons with energies up to approximately 8 MeV [5]. Although $0\nu\beta\beta$ decay experiments go to great lengths to minimize all actinide contamination, α decay is still observed on detector components. These α decays can initiate (α, n) reactions on ^{130}Te, ^{125}Te, and ^{18}O in SNO+ and CUORE. For SNO+, (α, n) reactions on ^{13}C are an additional accessible reaction channel. Neutrons from spontaneous fission of ^{238}U, although less likely, may also be produced inside the CUORE and SNO+ detectors.

In order to estimate the expected background in $0\nu\beta\beta$ decay experiments, the neutron-induced cross sections on the

*tornow@tunl.duke.edu

relevant isotopes must be known in the neutron energy range of interest. This has initiated a large effort by the Triangle Universities Nuclear Laboratory (TUNL) [6] and other experimental groups. A number of neutron-induced reactions have been measured on ^{76}Ge, including neutron capture [7], ^{76}Ge$(n, p)^{76}$Ga [8], and ^{76}Ge$(n, 2n)^{75}$Ge [9]. Similarly, the ^{136}Xe neutron capture cross section was measured in Ref. [10] and the ^{136}Xe$(n, 2n)^{135}$Xe cross section in Ref. [11]. Argon is an important component of $0\nu\beta\beta$ decay searches at the GERmanium Detector Array (GERDA) and the Large Enriched Germanium Experiment for Neutrinoless Double-Beta Decay (LEGEND). To aid in these efforts, the neutron capture [12] and ^{40}Ar$(n, p)^{40}$Cl [13] cross sections of argon have been measured. A number of recent experimental efforts have measured neutron-induced γ-ray production cross section on materials of relevance for $0\nu\beta\beta$ decay. This includes $\beta\beta$ decay nuclei ^{76}Ge [14–16] and ^{136}Xe [17–19]. In addition, there have been several studies on common detector shielding and structural components such as copper [20,21] and lead [22–24].

Focusing now on tellurium, the effect of detector and component activation by cosmic rays has been studied [25–27]. Several neutron-induced γ-ray production cross sections were measured during an extensive study using the GErmanium Array for Neutron-Induced Excitations (GEANIE) at the Los Alamos Neutron Science Center [28]. This work provides cross-section measurements for the first excited states of ^{126,128,130}Te from threshold to 200 MeV neutron energy. In addition, the 2607.33 keV γ-ray transition in ^{130}Te is also thoroughly measured. These are all transitions which decay directly to the ground state. There are additional γ-ray cascades, occurring from states in tellurium near the Q value for $0\nu\beta\beta$ decay of ^{130}Te at 2527.515 keV, which were not measured in Ref. [28]. In order to determine γ-ray production cross sections for these states, experiments were performed at TUNL. The following section, Sec. II, briefly describes the experimental setup. Section III focuses on the data-taking and data-analysis procedure. The results obtained in the present work are presented in Sec. IV. Finally, Sec. V provides a summary and concluding remarks.

II. EXPERIMENTAL SETUP

The ^{2}H$(d, n)^{3}$He reaction was used to produce monoenergetic neutrons with mean energies of 3.6, 4.5, 6.0, 8.0, and 10.0 MeV to cover the energy range of interest for (α, n) neutrons. The TUNL tandem accelerator was employed to accelerate pulsed (2.5 MHz) deuteron beams with pulse widths of approximately 2 ns onto a gas cell filled to 5 atm with high-purity deuterium gas [19]. Deuteron beam currents on target varied between 0.8 μA and 1.3 μA depending on deuteron energy and performance of the ion source. A schematic of the experimental setup is shown in Fig. 1. A massive shielding wall made of heavy metals, concrete, and polyethylene separates the neutron-production location from the tellurium target and detector location. Neutrons produced in a small forward-angle cone pass through a collimator made of copper and strike a 2.9 cm diameter and 0.6 cm thick natural tellurium disk with mass of 14.3 g, positioned at 0° at a

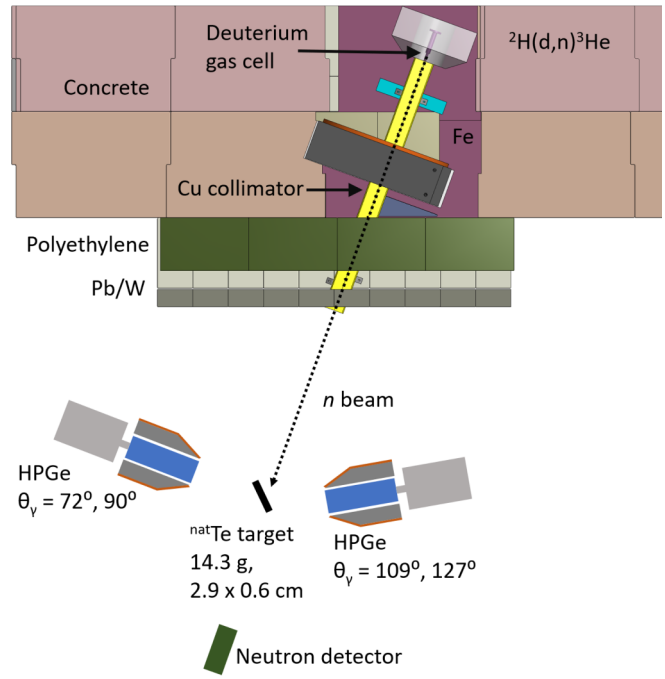

FIG. 1. Schematic of the experimental setup showing the neutron source, shielding wall, collimator, and the two clover HPGe detectors, which are positioned at $\theta_\gamma = 90^\circ$ and 127° relative to the incident pulsed neutron beam. The clover HPGe detectors measure γ rays originating from the neutron-illuminated natural tellurium target. A small liquid scintillator located downstream at 0° monitors the neutron beam. Data were also taken with the two clover HPGe detectors placed at $\theta_\gamma = 72^\circ$ and 109°.

distance of 175 cm from the deuterium gas cell. The tellurium disk is viewed by two high-purity germanium (HPGe) clover detectors. Two detector configurations were used. In the first configuration one detector was positioned at 90°, while the other was at 127° relative to the 0° neutron beam, as shown in Fig. 1. Here, the front face of the 90° detector was at a distance of 5.9 cm from the center of the tellurium disk, while for the 127° detector this distance had to be increased to 8.3 cm to avoid partial illumination of this detector by the 0° neutron beam. For the second configuration the HPGe detectors were positioned at 72° and 109° with distances of 8.2 cm and 5.3 cm, respectively, from the center of the tellurium disk. A 1.5″ × 1.5″ liquid scintillator neutron detector was placed downstream at 0° to monitor the neutron flux and the timing characteristics of the pulsed neutron beam. The actual neutron fluence was determined in separate experiments with the tellurium sample replaced by a natural iron disk of 2.9 cm diameter and thickness of 0.375 mm. The integrated deuteron beam current served as normalization between the tellurium and iron measurements. Normally, we would sandwich the tellurium sample between two iron foils for neutron fluence determination. To avoid interference of the ^{56}Fe γ-ray lines with the many γ-ray transitions of interest for tellurium, this approach had to be abandoned in this special case.

Traditionally $(n, n'\gamma)$ cross-section measurements are performed at a detector position near 127°, because in this special

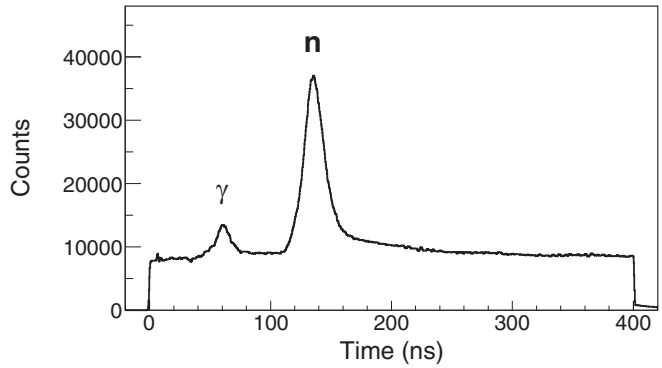

FIG. 2. Time-of-flight (TOF) spectrum generated by deuteron time pick-off signals and HPGe detector signals. Time increases from left to right. The strong peak is due to the neutron TOF between the deuterium gas cell and the tellurium target disk plus negligible TOF contributions from the deuteron beam (from the time pick-off unit to the deuterium gas cell) and from γ rays (generated in the tellurium target and detected in a HPGe detector).

case, angle-dependent terms in the differential cross-section expression are zero or very small, making it possible to determine the angle-integrated cross section in a single measurement at one angle [17,29]. Therefore, our three angular settings below 127° are not only intended to improve the statistical accuracy of the data, but also to check on the conjecture that the feeding of the state of interest from higher-lying excited states results in an approximately uniform decay γ-ray angular distribution.

III. DATA-TAKING AND ANALYSIS PROCEDURE

Time-of-flight (TOF) spectra were recorded with the start signal obtained from one of the clover-detector segments and the stop signal derived from the delayed signal of a capacitive time pick-off located just in front of the deuterium gas cell.

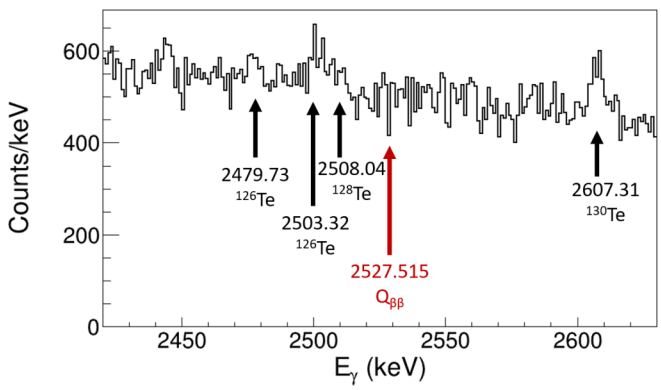

FIG. 3. Gamma-ray spectrum measured with 6 MeV neutrons in the energy region of interest for $0\nu\beta\beta$ decay of ^{130}Te. The arrow at 2527.515 keV indicates where a hypothetical $0\nu\beta\beta$ event would be located. In agreement with Ref. [30], the decay of the 2527.06 state in ^{130}Te is not observed, because there is no direct branching to the ground state. The ^{130}Te ground-state transition at 2607.31 keV is clearly seen, as is the ^{126}Te ground-state transition at 2503.2 keV, and less strong the ^{128}Te ground-state transition at 2508.04 keV.

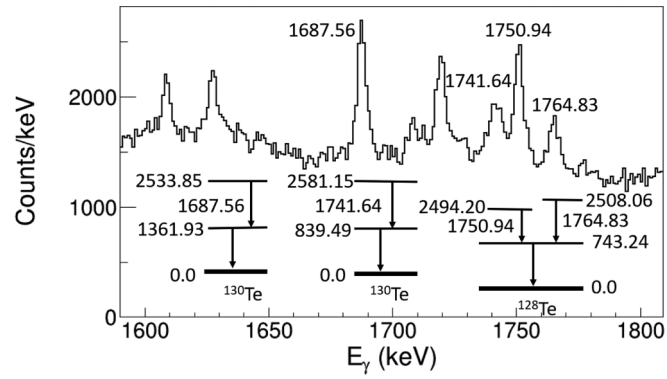

FIG. 4. Gamma-ray energy spectrum of one clover HPGe detector in the 1600 keV to 1800 keV energy range. The peaks labeled are from the decay of neutron-induced excitations of levels in ^{130}Te and ^{128}Te, respectively, as indicated in the partial level schemes below the peaks. The peaks not labeled are due to background. The incident neutron energy is 6 MeV.

One such spectrum is shown in Fig. 2 for an incident neutron energy of 6.0 MeV. The strong peak seen is due to the neutron flight time between the deuterium gas cell and the tellurium sample plus the negligible flight time of deexcitation γ rays between the tellurium sample and a clover detector segment, in addition to the very short flight time of the deuteron beam between the pick-off and the deuterium gas cell. The TOF peak from the γ-ray flash is visible to the left of the main neutron peak. The width of the TOF peak is typically 25 ns and is completely governed by the time resolution of the clover HPGe detectors. Gates set on the neutron peak and the random background were used to create two γ-ray spectra, labeled "true + accidental" and "accidental." After subtraction, the "true" γ-ray spectrum of interest was obtained. The four individual spectra of each clover detector were gain matched and added to provide one single spectrum for analysis.

Before presenting γ-ray spectra, we note that for ^{130}Te only the level located at 2527.06 keV is a potential background signal for CUORE, while for SNO+ an additional four levels between 2575.2 keV and 2648.57 keV are important [30]. For ^{128}Te there are no levels of concern for CUORE, but for

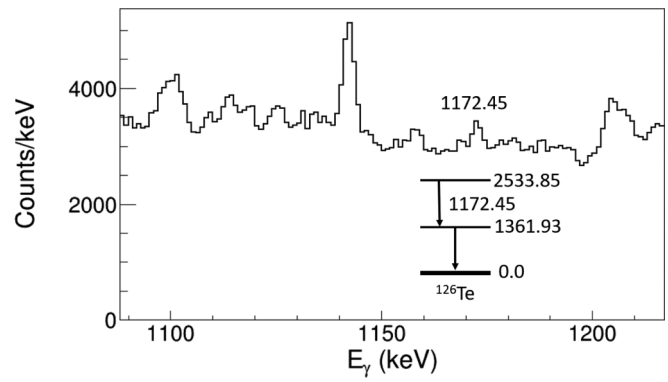

FIG. 5. Same as Fig. 4, but for the γ-ray energy region between approximately 1100 keV and 1200 keV, showing the deexcitation γ ray of 1172.45 keV, originating from the decay of the 2533.85 keV level in ^{126}Te.

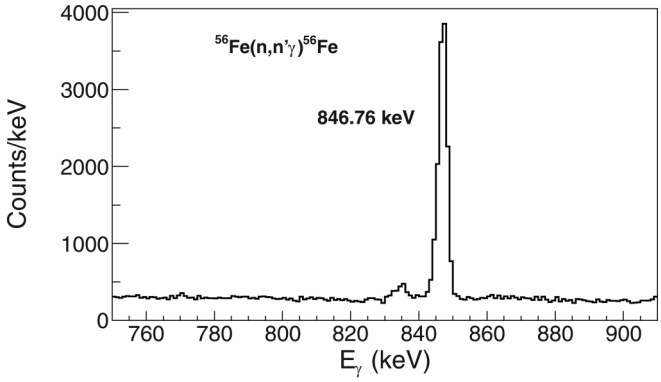

FIG. 6. Gamma-ray spectrum in the energy region between 750 keV and 900 keV obtained from 6 MeV neutron-induced excitation of the 846.78 keV level in ^{56}Fe used for neutron fluence determination.

SNO+ nine levels between 2494.20 keV and 2643.28 keV are a potential problem [31]. Finally, for ^{126}Te the level located at 2533.85 keV is of concern for CUORE, and SNO+ may be affected by eight additional levels between 2496.83 keV and 2640.4 keV [32]. The levels referred to above are based on the average energy resolution quoted by CUORE of (7.7 ± 0.5) keV, corresponding to $\Delta E/E \approx 0.3\%$ for its 988 TeO_2 bolometers, and the asymmetric energy region of interest for SNO+ between 2490 and 2650 keV.

Figure 3 shows a γ-ray spectrum obtained with 6 MeV neutrons in the energy region of interest for $0\nu\beta\beta$ of ^{130}Te. Clearly, in the energy region of $Q_{\beta\beta} = 2527.515$ keV there is no indication of a peak above background. According to Ref. [30], the ^{130}Te level at 2527.06 keV does not decay directly to the ground state, as confirmed by the present measurement. The ^{130}Te level at 2607.33 keV, however, does decay to the ground state, and therefore is clearly visible in Fig. 3. Also shown in Fig. 3 are the ground-state transitions of ^{126}Te and ^{128}Te at 2503.55 keV and 2508.06 keV, respectively. In Ref. [2] this energy region is dominated by the ^{60}Co sum peak at 2507.5 keV. Figure 3 exhibits a peak at 2480 keV.

TABLE I. Mean neutron energy and associated energy spread, HPGe detector angle settings, ^{56}Fe$(n, n'\gamma)$ reference cross section utilized [33], incident pulsed deuteron beam current, and data-acquisition time used in the present work.

$E_n \pm \Delta E_n$ (MeV)	Angles (°)	^{56}Fe$(n, n'\gamma)$ (b)	I_d (μA)	Measurement time (h)
3.6 ± 0.7	90, 127	1.30 ± 0.10	0.9	48
3.6 ± 0.7	72, 109	1.30 ± 0.10	0.8	60
4.5 ± 0.7	90, 127	1.40 ± 0.11	1.0	48
4.5 ± 0.7	72, 109	1.40 ± 0.11	1.1	45
6.0 ± 0.4	90, 127	1.49 ± 0.12	1.2	24
6.0 ± 0.4	72, 109	1.49 ± 0.12	1.1	24
8.0 ± 0.2	90, 127	1.33 ± 0.11	1.3	18
8.0 ± 0.2	72, 109	1.33 ± 0.11	1.0	20
10.0 ± 0.2	90, 127	1.35 ± 0.11	1.1	21
10.0 ± 0.2	72, 109	1.35 ± 0.11	1.0	21

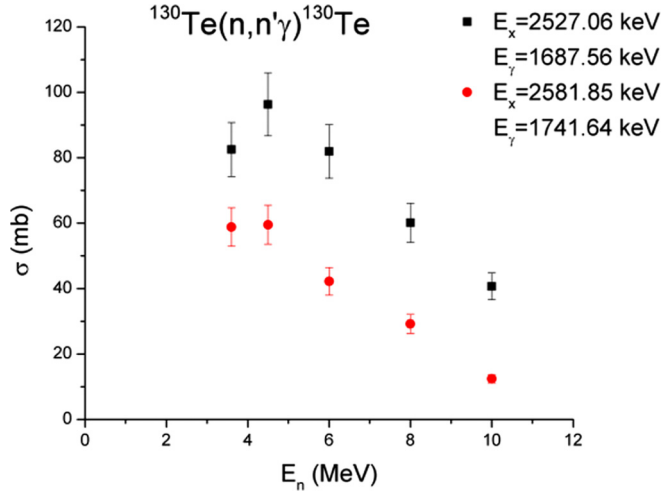

FIG. 7. Neutron-induced production cross sections of 1687.56 keV and 1741.64 keV γ rays, resulting from the decay of the 2527.06 keV and 2581.85 keV levels of ^{130}Te, as a function of incident neutron energy.

Interestingly, Ref. [2] refers to an unidentified background peak at 2480 keV. According to Ref. [32], there is a state in ^{126}Te at 2479.73, which however does not decay directly to the ground state. Furthermore, Ref. [32] has a question mark attached to this state, although it has been identified in ^{126}Te$(n, n'\gamma)$ ^{126}Te and ^{126}Te(d, d') ^{126}Te experiments.

Figure 4 presents a γ-ray spectrum obtained at $E_n = 6.0$ MeV in the energy range between 1600 and 1800 keV. The peaks of interest belonging to ^{130}Te and ^{128}Te are marked. The insets show the partial level schemes of interest for the transitions observed. The peaks without labels are background peaks. Figure 5 displays a γ-ray spectrum of interest for ^{126}Te, with the partial level scheme shown again in the

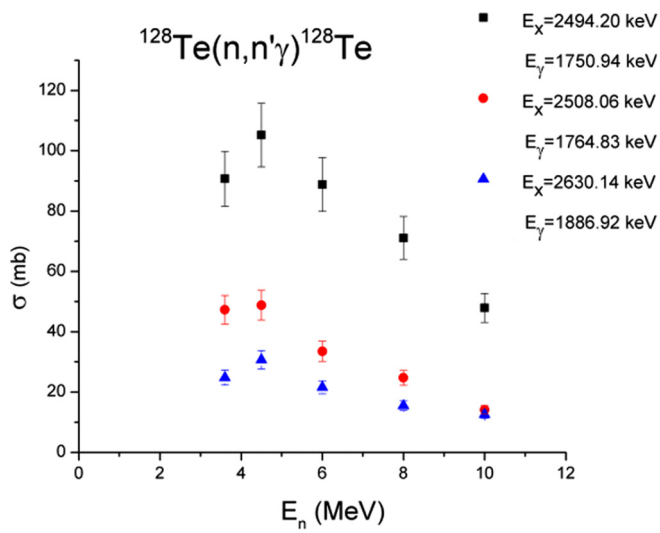

FIG. 8. Neutron-induced production cross sections of 1750.94 keV, 1764.83 keV, and 1886.92 keV γ rays, resulting from the decay of the 2494.20 keV, 2508.06 keV, and 2630.14 keV levels of ^{128}Te, as a function of incident neutron energy.

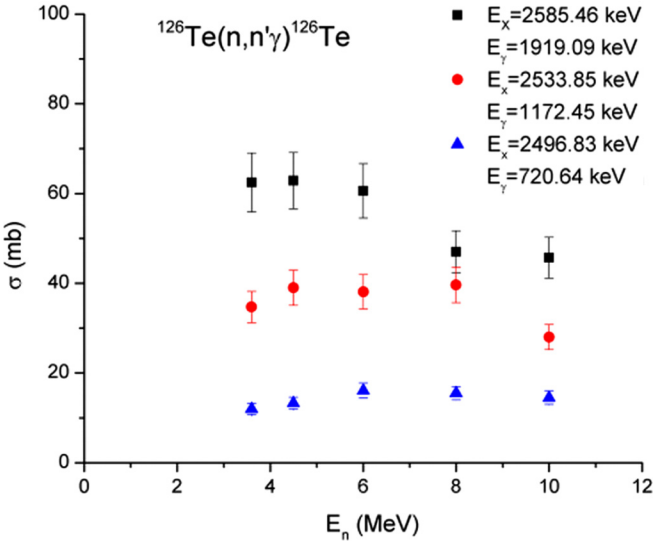

FIG. 9. Neutron-induced production cross sections of 1919.09 keV, 1172.45 keV, and 720.64 keV γ rays, resulting from the decay of the 2585.46 keV, 2533.85 keV, and 2496.83 keV levels of ^{126}Te, as a function of incident neutron energy.

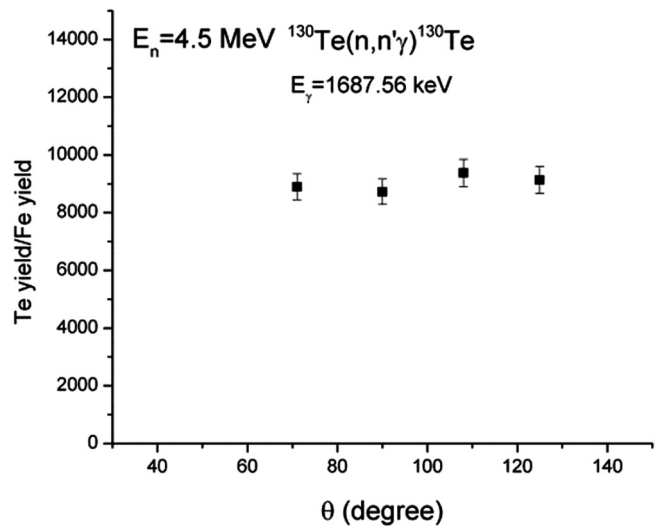

FIG. 10. Angular dependence of the ratio of ^{130}Te and ^{56}Fe yields measured with 4.5 MeV incident neutrons. Here, the decay γ rays of the 2527.06 keV level in ^{130}Te and the 846.78 keV level in ^{56}Fe were used.

inset. Finally, Fig. 6 gives a γ-ray spectrum obtained with the iron target in the neutron beam. The strong γ-ray line at 846.76 keV used for cross-section normalization is clearly visible.

The efficiencies of the clover HPGe detectors were measured with a mixed γ-ray source containing eight isotopes ranging from ^{241}Am ($E_\gamma = 59.5$ keV) to ^{88}Y ($E_\gamma = 1836.1$ keV), covering the entire energy range of cascade γ rays studied in the present work. This source was placed at the location of the tellurium target to obtain an accurate determination of the efficiencies for our experimental setup. Small corrections were applied to account for the different size of the tellurium target and the γ-ray calibration source. Corrections were also applied to correct for the dead time of the data-acquisition system.

Table I provides information on the neutron energy and associated energy spread, clover HPGe detector angle settings, average pulsed deuteron beam current, and data-acquisition time used in the present work.

IV. RESULTS

The neutron fluence to which the tellurium sample was exposed was calculated from the number of ^{56}Fe nuclei, the yield in the 846.76 keV peak, $I_\gamma = 1$ [34], a small self-attenuation correction, the integrated deuteron beam current ratio for the tellurium and iron runs, the cross-section value for the ^{56}Fe$(n, n'\gamma)^{56}$Fe reaction of Beyer *et al.* [33], and the clover HPGe detector efficiency. Using this information and the number of ^{130}Te, ^{128}Te, and ^{126}Te nuclei in the natural tellurium sample, the yields in the peaks of interest, and the associated γ-ray detection efficiencies (again after self-absorption corrections), the γ-ray production cross sections $\sigma_{^{130}\mathrm{Te}}$, $\sigma_{^{128}\mathrm{Te}}$, and $\sigma_{^{126}\mathrm{Te}}$ were computed. They are plotted in Figs. 7–9 for the ^{130}Te$(n, n'\gamma)^{130}$Te, ^{128}Te$(n, n'\gamma)^{128}$Te, and ^{126}Te$(n, n'\gamma)^{126}$Te reactions.

We start the discussion of our results by first noticing the uniform angular distribution obtained, for example at 4.5 MeV for the relative yield of the 1687.56 keV transition, as shown in Fig. 10. Such a uniform angular distribution is expected

TABLE II. Gamma-ray production cross-section results for the various γ rays measured in the present work.

	^{130}Te	^{130}Te	^{128}Te	^{128}Te	^{128}Te	^{126}Te	^{126}Te	^{126}Te
E_γ	1687.56 keV	1741.64 keV	1750.94 keV	1764.83 keV	1886.92 keV	1919.09 keV	1172.45 keV	720.64 keV
E_x	2527.06 keV	2581.85 keV	2494.20 keV	2508.06 keV	2630.14 keV	2585.46 keV	2533.85 keV	2496.83 keV
E_n (MeV)	σ (mb)	σ (mb)	σ (mb)	σ (mb)	σ (mb)	σ (mb)	σ (mb)	σ (mb)
3.6	82.5 ± 8.3	58.8 ± 5.9	90.7 ± 9.2	47.3 ± 4.8	24.8 ± 2.5	65.5 ± 6.6	34.7 ± 3.5	12 ± 1.2
4.5	96.3 ± 9.2	59.5 ± 5.7	105.2 ± 10.1	48.8 ± 4.7	30.7 ± 2.9	62.9 ± 6	39 ± 3.7	13.3 ± 1.3
6	81.9 ± 7.5	42.2 ± 3.9	88.8 ± 8.2	33.5 ± 3.1	21.7 ± 2	60.6 ± 5.6	38.1 ± 3.5	16.1 ± 1.5
8	60.1 ± 5.3	29.2 ± 2.6	71.1 ± 6.3	24.7 ± 2.2	15.5 ± 1.4	47 ± 4.2	39.6 ± 3.5	15.5 ± 1.4
10	40.7 ± 3.6	12.4 ± 1.1	47.9 ± 4.2	14.1 ± 1.2	12.6 ± 1.1	45.7 ± 4	28 ± 2.5	14.5 ± 1.3

TABLE III. Uncertainty budget.

Source	Te	Fe
Counting statistics	1.5%–5%	0.7%–1.5%
Reference cross section		8.0%
HPGe detector efficiency	3.1%	3.1%
Self-absorption of γ rays	<1%	<0.5%
Target mass	1.0%	<0.5%

from the various γ-ray transitions of different multipolarities feeding the associated 2527.06 keV level. The same argument holds for the 846.76 keV transition in ^{56}Fe studied by Beyer *et al.* [29].

Now concentrating on ^{130}Te (Fig. 7), the tellurium isotope with the largest natural abundance of 34.08%, and the main $0\nu\beta\beta$ candidate studied at CUORE and SNO+, we note that the 1687.56 keV transition originating from the decay of the 2527.06 keV level is the second largest Te cross section measured in the present work. It peaks near 5 MeV with close to 100 mb and then drops off to 40 mb at 10 MeV, the highest neutron energy used in the present work. If the following 839.49 keV γ ray is also detected in the same 750 g TeO_2 crystal at CUORE, or in the vicinity of the 1687.56 keV deposition in the liquid scintillator at SNO+, a perfect match with the $0\nu\beta\beta$ decay energy of 2527.510 keV for ^{130}Te would be achieved, making it impossible to distinguish the potential $0\nu\beta\beta$ event of interest from this neutron-induced background event. The 2527.06 keV level is the only ^{130}Te level of concern for CUORE, while for SNO+ the level at 2581.85 keV with its decay γ rays of 1741.64 keV and 839.49 keV causes an additional problem, although the associated cross section for the 1741.64 keV transition is somewhat lower, peaking at 60 mb and exhibiting the same energy dependence as observed for the 1687.56 keV γ-ray transition.

Turning our discussion to ^{128}Te with its natural abundance of 31.74%, we reiterate that only SNO+ is affected by neutron inelastic scattering events on ^{128}Te. Figure 8 presents γ-ray production cross sections for deexcitation γ rays at 1750.94 keV, 1764.83 keV, and 1886.92 keV, originating from ^{128}Te levels at 2494.20 keV, 2508.06 keV, and 2630.14 keV, respectively [31]. The production cross section of the 1750.94 keV transition peaks just above 100 mb at 4.5 MeV and then follows the energy dependence already seen in Fig. 7 for ^{130}Te. The other two transitions shown in Fig. 8 have a factor of two to four smaller cross sections.

Finally, we turn our attention to ^{126}Te with its natural abundance of 18.84%. As can be seen from Fig. 9, the deexcitation 1172.45 keV γ rays originating from the decay of the 2533.85 keV level are a potential problem for CUORE with a cross section of just below 40 mb. The other two γ-ray transitions at 1909.09 keV and 720.64 keV affect only SNO+ and have cross-section values of approximately 55 mb and 15 mb, respectively.

Table II gives our results in numerical form. Here the uncertainties assigned are governed by statistics, and include the 3.1% uncertainty in the γ-ray detection efficiency and the 8% uncertainty in the neutron fluence determination. Details are given in Table III.

V. SUMMARY AND CONCLUSIONS

Monoenergetic neutron-induced γ-ray production cross sections have been measured at five energies between 3.6 and 10 MeV for the reactions ^{126,128,130}Te$(n,n'\gamma)^{126,128,130}$Te using natural tellurium targets. These data, combined with those of Ref. [28], provide valuable information on potential backgrounds in the $0\nu\beta\beta$ decay searches of ^{130}Te at CUORE and SNO+, where natural tellurium is used. The neutron energies were chosen to represent the energy range most important for the production of γ rays that can mimic the $0\nu\beta\beta$ signal of interest. It was found that the excitation of the ^{130}Te level at 2527.06 keV has the very large cross section of 100 mb at 4.5 MeV. If the associated two successive decay γ rays with energies of 1687.56 keV and 839.494 keV are detected in one of the TeO_2 crystals at CUORE or in a small volume of the large scintillator at SNO+, an unfortunately prefect match is created with the ^{130}Te $0\nu\beta\beta$ Q value of 2527.510 keV, making it impossible to distinguish a potential $0\nu\beta\beta$ event from neutron-induced background. For both CUORE and SNO+, the excitation of the 2533.85 keV level in ^{126}Te with a production cross section of 40 mb may also cause a problem. For SNO+ with its inferior energy resolution compared to CUORE, a total of six additional excited levels in ^{130}Te, ^{128}Te, and ^{126}Te are important, clearly showing the need for excellent energy resolution in $0\nu\beta\beta$ searches. The 2527.06 keV level in ^{130}Te, however, clearly shows that this is only a necessary, but not sufficient, condition, because a completely actinide-free $0\nu\beta\beta$ detector is an impossible goal to achieve, and a perfect veto against cosmic-ray-produced neutrons within the detector or its shielding cannot be built either. Therefore, the present data are an important contribution to estimate potential backgrounds in $0\nu\beta\beta$ decay searches of ^{130}Te.

ACKNOWLEDGMENTS

This work was supported in part by the US Department of Energy, Office of Nuclear Physics, under Grant No. DE-FG02-97ER41033. M.F.K. was supported by the National Science Foundation under Grant No. PHY-1614348. Contributions from Krishichayan, TUNL, are greatly appreciated.

[1] F. T. Avignone, S. R. Elliott, and J. Engel, Rev. Mod. Phys. **80**, 481 (2008).
[2] D. Q. Adams *et al.* (CUORE Collaboration), Phys. Rev. Lett. **124**, 122501 (2020).
[3] S. Andringa *et al.* (SNO+ Collaboration), Adv. High Energy Phys. **2016**, 21 (2016).
[4] D.-M. Mei and A. Hime, Phys. Rev. D **73**, 053004 (2006).

[5] V. Kudryavtsev, P. Zakhary, and B. Easeman, Nucl. Instrum. Methods Phys. Res. Sect. A **972**, 164095 (2020).
[6] W. Tornow and M. Bhike, EPJ Web Conf. **93**, 03001 (2015).
[7] M. Bhike, B. Fallin, Krishichayan, and W. Tornow, Phys. Lett. B **741**, 150 (2015).
[8] W. Tornow, M. Bhike, B. Fallin, and Krishichayan, Phys. Rev. C **93**, 014614 (2016).
[9] M. Bhike, Krishichayan, and W. Tornow, Phys. Rev. C **95**, 054605 (2017).
[10] J. B. Albert, S. J. Daugherty, T. N. Johnson, T. O'Conner, L. J. Kaufman, A. Couture, J. L. Ullmann, and M. Krtička, Phys. Rev. C **94**, 034617 (2016).
[11] C. Bhatia, S. W. Finch, M. E. Gooden, and W. Tornow, Phys. Rev. C **87**, 011601(R) (2013).
[12] V. Fischer, L. Pagani, L. Pickard, A. Couture, S. Gardiner, C. Grant, J. He, T. Johnson, E. Pantic, C. Prokop, R. Svoboda, J. Ullmann, and J. Wang (ACED Collaboration), Phys. Rev. D **99**, 103021 (2019).
[13] C. Bhatia, S. W. Finch, M. E. Gooden, and W. Tornow, Phys. Rev. C **86**, 041602(R) (2012).
[14] C. Rouki, A. R. Domula, J. C. Drohé, A. J. Koning, A. J. M. Plompen, and K. Zuber, Phys. Rev. C **88**, 054613 (2013).
[15] A. Domula, D. Gehre, K. Zuber, J. Drohé, N. Nankov, A. Plompen, C. Rouki, M. Stanoiu, A. Klix, A. Buffler, D. Geduld, F. Smit, C. Vermeulen, P. Maleka, R. Newman, R. Nolte, and A. Wallner, Nucl. Data Sheets **120**, 44 (2014).
[16] B. P. Crider, E. E. Peters, J. M. Allmond, M. T. McEllistrem, F. M. Prados-Estévez, T. J. Ross, J. R. Vanhoy, and S. W. Yates, Phys. Rev. C **92**, 034310 (2015).
[17] E. E. Peters, T. J. Ross, S. H. Liu, M. T. McEllistrem, and S. W. Yates, Phys. Rev. C **95**, 014325 (2017).
[18] S. J. Daugherty, J. B. Albert, L. J. Kaufman, M. Devlin, N. Fotiades, R. O. Nelson, and M. Krtička, Phys. Rev. C **98**, 064606 (2018).
[19] M. Bhike, J. Esterline, B. Fallin, S. Finch, M. Gooden, and W. Tornow, J. Phys. G: Nucl. Part. Phys. **45**, 125101 (2018).
[20] M. S. Boswell, S. R. Elliott, D. V. Perepelitsa, M. Devlin, N. Fotiades, R. O. Nelson, T. Kawano, and V. E. Guiseppe, Phys. Rev. C **87**, 064607 (2013).
[21] M. Gooden, B. Fallin, S. Finch, J. Kelley, C. Howell, G. Rusev, A. Tonchev, W. Tornow, and V. Stanislav, Nucl. Data Sheets **119**, 121 (2014).
[22] D.-M. Mei, S. R. Elliott, A. Hime, V. Gehman, and K. Kazkaz, Phys. Rev. C **77**, 054614 (2008).
[23] V. E. Guiseppe, M. Devlin, S. R. Elliott, N. Fotiades, A. Hime, D.-M. Mei, R. O. Nelson, and D. V. Perepelitsa, Phys. Rev. C **79**, 054604 (2009).
[24] A. Negret, C. Borcea, and A. J. M. Plompen, Phys. Rev. C **88**, 027601 (2013).
[25] A. Barghouty, C. Brofferio, S. Capelli, M. Clemenza, O. Cremonesi, S. Cebrián, E. Fiorini, R. Haight, E. Norman, M. Pavan, E. Previtali, B. Quiter, M. Sisti, A. Smith, and S. Wender, Nucl. Instrum. Methods Phys. Res. Sect. B **295**, 16 (2013).
[26] B. S. Wang, E. B. Norman, N. D. Scielzo, A. R. Smith, K. J. Thomas, and S. A. Wender, Phys. Rev. C **92**, 024620 (2015).
[27] S. Cebrián, Universe **6**, 162 (2020).
[28] M. J. Dolinski, Ph.D. thesis, University of California, Berkeley, 2008.
[29] R. Beyer, M. Dietz, D. Bemmerer, A. R. Junghans, T. K. R. Massarczyk, S. Müller, K. Schmidt, R. Schwengner, T. Szücs, M. P. Takács, and A. Wagner, Eur. Phys. J. A **54**, 58 (2018).
[30] B. Singh, Nucl. Data Sheets **93**, 33 (2001).
[31] Z. Elekes and J. Timar, Nucl. Data Sheets **129**, 191 (2015).
[32] J. Katakura and K. Kitao, Nucl. Data Sheets **97**, 765 (2002).
[33] R. Beyer, R. Schwengner, R. Hannaske, A. Junghans, R. Massarczyk, M. Anders, D. Bemmerer, A. Ferrari, A. Hartmann, T. Kögler, M. Röder, K. Schmidt, and A. Wagner, Nucl. Phys. A **927**, 41 (2014).
[34] H. Junde, H. Su, and Y. Dong, Nucl. Data Sheets **112**, 1513 (2011).